




# Behavioral and Cognitive Improvement Induced by Novel Imidazoline I<sub>2</sub> Receptor Ligands in Female SAMP8 Mice

Christian Griñán-Ferré<sup>1</sup> · Foteini Vasilopoulou<sup>1</sup> · Sònia Abás<sup>2</sup> · Sergio Rodríguez-Arévalo<sup>2</sup> · Andrea Bagán<sup>2</sup> · Francesc X. Sureda<sup>3</sup> · Belén Pérez<sup>4</sup> · Luis F. Callado<sup>5,6</sup> · Jesús A. García-Sevilla<sup>7</sup> · M. Julia García-Fuster<sup>7</sup> · Carmen Escolano<sup>2</sup> · Mercè Pallàs<sup>1</sup> 

Published online: 20 November 2018

© The American Society for Experimental NeuroTherapeutics, Inc. 2018

## Abstract

As populations increase their life expectancy, age-related neurodegenerative disorders such as Alzheimer's disease have become more common. I<sub>2</sub>-Imidazoline receptors (I<sub>2</sub>-IR) are widely distributed in the central nervous system, and dysregulation of I<sub>2</sub>-IR in patients with neurodegenerative diseases has been reported, suggesting their implication in cognitive impairment. This evidence indicates that high-affinity selective I<sub>2</sub>-IR ligands potentially contribute to the delay of neurodegeneration. *In vivo* studies in the female senescence accelerated mouse-prone 8 mice have shown that treatment with I<sub>2</sub>-IR ligands, **MCR5** and **MCR9**, produce beneficial effects in behavior and cognition. Changes in molecular pathways implicated in oxidative stress, inflammation, synaptic plasticity, and apoptotic cell death were also studied. Furthermore, treatments with these I<sub>2</sub>-IR ligands diminished the amyloid precursor protein processing pathway and increased Aβ degrading enzymes in the hippocampus of SAMP8 mice. These results collectively demonstrate the neuroprotective role of these new I<sub>2</sub>-IR ligands in a mouse model of brain aging through specific pathways and suggest their potential as therapeutic agents in brain disorders and age-related neurodegenerative diseases.

**Keywords** Imidazoline I<sub>2</sub> receptors · (2-imidazolin-4-yl)phosphonates · Behavior · Cognition · Neurodegeneration · Neuroprotection · Aging

## Introduction

Imidazoline receptors (non-adrenergic receptors for imidazolines) [1] have been identified as a promising biological target that deserves further investigation using

multidisciplinary approaches to build a comprehensive understanding of their pharmacological possibilities. To date, three main imidazoline receptors, I<sub>1</sub>-, I<sub>2</sub>- and I<sub>3</sub>-IR, have been identified as binding sites that recognize different radiolabeled ligands involving different locations and physiological

Christian Griñán-Ferré and Foteini Vasilopoulou contributed equally to this work.

**Electronic supplementary material** The online version of this article (<https://doi.org/10.1007/s13311-018-00681-5>) contains supplementary material, which is available to authorized users.

✉ Mercè Pallàs  
pallas@ub.edu

<sup>1</sup> Pharmacology Section, Department of Pharmacology, Toxicology and Medicinal Chemistry, Faculty of Pharmacy and Food Sciences, and Institut de Neurociències, University of Barcelona, Av. Joan XXIII, 27-31, 08028 Barcelona, Spain

<sup>2</sup> Laboratory of Medicinal Chemistry (Associated Unit to CSIC), Department of Pharmacology, Toxicology and Medicinal Chemistry, Faculty of Pharmacy and Food Sciences, and Institute of Biomedicine (IBUB), University of Barcelona, Av. Joan XXIII, 27-31, 08028 Barcelona, Spain

<sup>3</sup> Pharmacology Unit, Faculty of Medicine and Health Sciences, University of Rovira and Virgili, C./St. Llorenç 21, 43201 Reus, Tarragona, Spain

<sup>4</sup> Department of Pharmacology, Therapeutic and Toxicology, Autonomous University of Barcelona, 08193 Barcelona, Spain

<sup>5</sup> Department of Pharmacology, University of the Basque Country, UPV/EHU, 48940 Leioa, Bizkaia, Spain

<sup>6</sup> Centro de Investigación Biomédica en Red de Salud Mental, CIBERSAM, Leioa, Spain

<sup>7</sup> Laboratory of Neuropharmacology, IUNICS and IdISBa, University of the Balearic Islands (UIB), Cra. Valldemossa km 7.5, 07122 Palma de Mallorca, Spain

functions [2–4]. The pharmacological characterization of I<sub>1</sub>-IR is understood the best, and they are used in the antihypertensive drugs moxonidine [5] or rilmenidine [6]. To date, I<sub>2</sub>-IR have not been structurally described, although García-Sevilla's group has defined distinct binding proteins corresponding to subgroups of I<sub>2</sub>-IR sites [7]. I<sub>2</sub>-IR are involved in analgesia [8], glial tumors [9], inflammation [10] and a plethora of brain disorders, such as AD [11, 12], Parkinson's disease (PD) [13], and different psychiatric disorders [14–16]. The efficacy of the analgesic CR4056 in osteoarthritis has advanced this compound in the first-in-class I<sub>2</sub>-IR ligand to achieve phase II clinical trials [17]. I<sub>2</sub>-IR are widely distributed in the CNS, bind imidazoline-based compounds [18, 19], such as idazoxan or valdemossine [20], and have been associated with the catalytic site of monoamine oxidase enzyme (MAO) [21]. A neuroprotective role for I<sub>2</sub>-IR was described through the pharmacological activities observed for their ligands [22]. Idazoxan reduced neuron damage in the hippocampus after global ischemia in the rat brain [23] and agmatine, identified as the endogenous I<sub>2</sub>-IR ligand [24], has demonstrated modulatory actions in several neurotransmitters that produce neuroprotection both *in vitro* and in rodent models [25]. The compelling evidence has demonstrated that other selective I<sub>2</sub>-IR ligands (Fig. 1) provide benefits such as being neuroprotective against cerebral ischemia *in vivo* [26, 27], inducing beneficial effects in several models of chronic opioid therapy, leading to neuroprotection by direct blocking of *N*-methyl-D-aspartate receptor (NMDA) mediated intracellular [Ca<sup>2+</sup>] influx [28], or provoking morphological/biochemical changes in astroglia that are neuroprotective after neonatal axotomy [22].

At a cellular level, I<sub>2</sub>-IR are situated in the outer membrane of the mitochondria in astrocytes [29], and a direct physiological function of glial I<sub>2</sub>-imidazoline preferring sites that regulate the level of the astrocyte marker glial fibrillary acidic protein (*Gfap*) has been proposed [30]. In addition, astrogliosis is a pathophysiological trend in brain neurodegeneration as in AD [31]. The density of I<sub>2</sub>-IR is markedly increased in the brains of patients with AD [13], and in gliosis associated with brain injury [32].

The pharmacological characterization of these receptors relies on the discovery of selective I<sub>2</sub>-IR ligands devoid of a

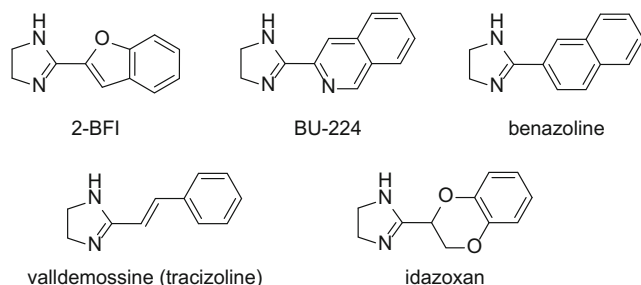


Fig. 1. Representative I<sub>2</sub>-IR ligands

high affinity for I<sub>1</sub>-IR and  $\alpha_2$ -adrenoceptors. The reported I<sub>2</sub>-IR ligands are structurally restricted, featuring rigid substituted pattern imidazolines, and most of which are not entirely selective and thus interact with  $\alpha$ -adrenoceptors [19], which causes side effects [33]. Our chemistry program aimed to find new selective I<sub>2</sub>-IR ligands to increase the arsenal of pharmacological tools to exploit the therapeutic potential of I<sub>2</sub>-IR in neuroprotection.

We have recently synthesized a series of new chemical scaffolds, 2-(imidazolin-4-yl)phosphonates [34], by an isocyanide-based multicomponent reaction under microwave irradiation to avoid using solvents. The experimental synthetic conditions fulfill the principles of green chemistry, giving access to novel compounds with high selectivity and affinity for I<sub>2</sub>-IR. Among them, we tested MCR5 [diethyl (1-(3-chloro-4-fluorobenzyl)-5,5-dimethyl-4-phenyl-4,5-dihydro-1*H*-imidazol-4-yl)phosphonate] in a previous work to demonstrate its neuroprotective and analgesic effects, and it showed promising results in models of brain damage [35]. In particular, mechanisms of neuroprotection related to regulating apoptotic pathways or inhibiting p35 cleavage mediated by this new active compound have been found. In the present work, we explored the behavioral and cognitive status, including molecular changes associated with age and neurodegenerative processes, presented by SAMP8 mice when treated with the new highly selective I<sub>2</sub>-IR ligands MCR5 and MCR9 [methyl 1-(3-chloro-4-fluorobenzyl)-5,5-dimethyl-4-phenyl-4,5-dihydro-1*H*-imidazole-4-carboxylate] (Fig. 2). SAMP8 is a naturally occurring mouse strain that displays a phenotype of accelerated aging with cognitive decline, as observed in AD, and is widely used as a feasible rodent model of cognitive dysfunction [36]. To the best of our knowledge, this manuscript reports the first study that includes cognitive and behavioral parameters of novel I<sub>2</sub>-IR ligands in a well-characterized animal model for studying brain aging and neurodegeneration.

## Material and Methods

### Synthesis of I<sub>2</sub>-IR Ligands MCR5 and MCR9

The compounds were prepared using our previously optimized conditions [34]. I<sub>2</sub>-IR pK<sub>i</sub> for MCR5 and MCR9 were

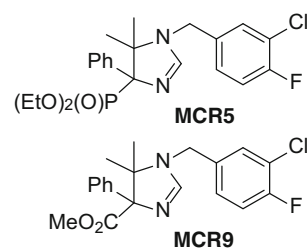


Fig. 2. Structure of I<sub>2</sub>-IR ligands MCR5 and MCR9

determined as  $9.42 \pm 0.16$  nM and  $8.85 \pm 0.21$  nM, respectively, showing that both compounds also had high selectivity against  $\alpha_2$  adrenergic receptors (457 and 1862, respectively) [35].

### The Blood-Brain Barrier (BBB) Determination Method

The *in vitro* permeability ( $P_e$ ) of the novel compounds through a lipid extract of the porcine brain was determined using a mixture of PBS/EtOH 70:30. The concentration of drugs was determined using a UV/VIS (250–500 nm) plate reader. Assay validation was carried out by comparing the experimental and reported permeability values of 14 commercial drugs (see supporting information), which provided a good linear correlation:  $P_e(\text{exp}) = 1.003 P_e(\text{lit}) - 0.783$  ( $R^2 = 0.93$ ). Using this equation and the limits established by Di et al. [37] for BBB permeation, the following ranges of permeability were established:  $P_e(10^{-6} \text{ cm}\cdot\text{s}^{-1}) > 5.18$  for compounds with high BBB permeation (CNS+);  $P_e(10^{-6} \text{ cm}\cdot\text{s}^{-1}) < 2.06$  for compounds with low BBB permeation (CNS-); and  $5.18 > P_e(10^{-6} \text{ cm}\cdot\text{s}^{-1}) > 2.06$  for compounds with uncertain BBB permeation (CNS±).

### Measurements of Hypothermic Effects

For this study, 25 adult male CD-1 mice (30–40 g) bred in the animal facility at the University of the Balearic Islands were used. Mice were housed in standard cages under defined environmental conditions (22°C, 70% humidity, and a 12-h light/dark cycle, lights on at 8:00 AM) and with free access to a standard diet and tap water. Experimental procedures followed the ARRIVE [38] and standard ethical guidelines (European Communities Council Directive 86/609/EEC and Guidelines for the Care and Use of Mammals in Neuroscience and Behavioral Research, National Research Council 2003) and were approved by the Local Bioethics Committee (UIB-

CAIB). All efforts were made to minimize the number of mice used and their suffering.

Mice were handled and weighed by the same person for 2 days so they could habituate to the experimenter before any experimental procedures were initiated. For the acute treatment, mice received a single dose of **MCR9** (20 mg/kg, i.p.,  $n=6$ ) or vehicle (a mixture of equal parts of DMSO and saline, i.p.,  $n=7$ ). For the repeated treatment, mice were treated daily with **MCR9** (20 mg/kg, i.p.,  $n=6$ ) or vehicle (a mixture of equal parts of DMSO and saline, i.p.,  $n=6$ ) for 5 consecutive days. The hypothermic effect of compound **MCR9** was evaluated by measuring rectal temperature before any drug treatment (basal value) and 1 h after drug injection by a rectal probe connected to a digital thermometer (compact LCD thermometer, SA880-1M, RS, Corby, UK). Mice were sacrificed immediately after the last measurement of rectal temperature.

### SAMP8 Mouse *In Vivo* Experiments

SAMP8 female mice ( $n=26$ ) (12 months old) were used to carry out cognitive and molecular analyses. We divided these animals randomly into three groups: SAMP8 Control ( $n=10$ ) and SAMP8 treated with  $I_2$ -IR ligands (**MCR5**,  $n=8$  and **MCR9**,  $n=8$ ). Animals had free access to food and water and were kept under standard temperature conditions ( $22 \pm 2^\circ\text{C}$ ) and a 12-h light/dark cycle (300 lux/0 lux). **MCR5** and **MCR9** (5 mg/Kg/day) were dissolved in 1.8% 2-hydroxypropyl- $\beta$ -cyclodextrin and administered through drinking water for 4 weeks. Water consumption was controlled each week, and  $I_2$ -IR ligand concentrations were adjusted accordingly to reach the optimal dose.

Studies and procedures involving mice brain dissection and subcellular fractionation were performed by the ARRIVE [38] and international guidelines for the care and use of laboratory animals (see above) and approved by the Ethics Committee for Animal Experimentation at the University of Barcelona.

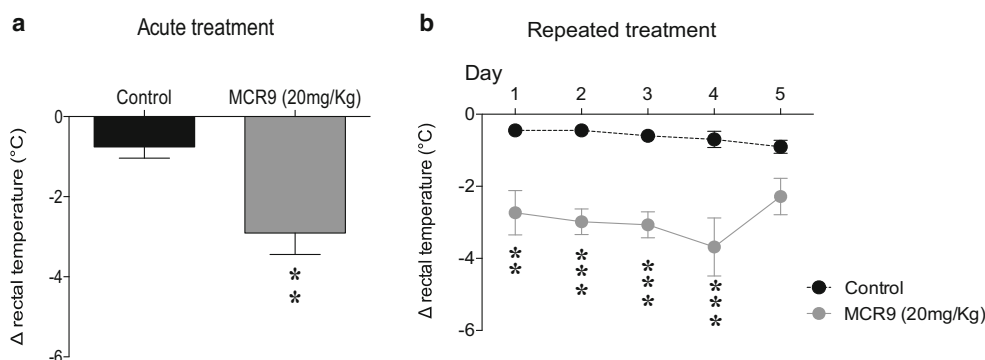
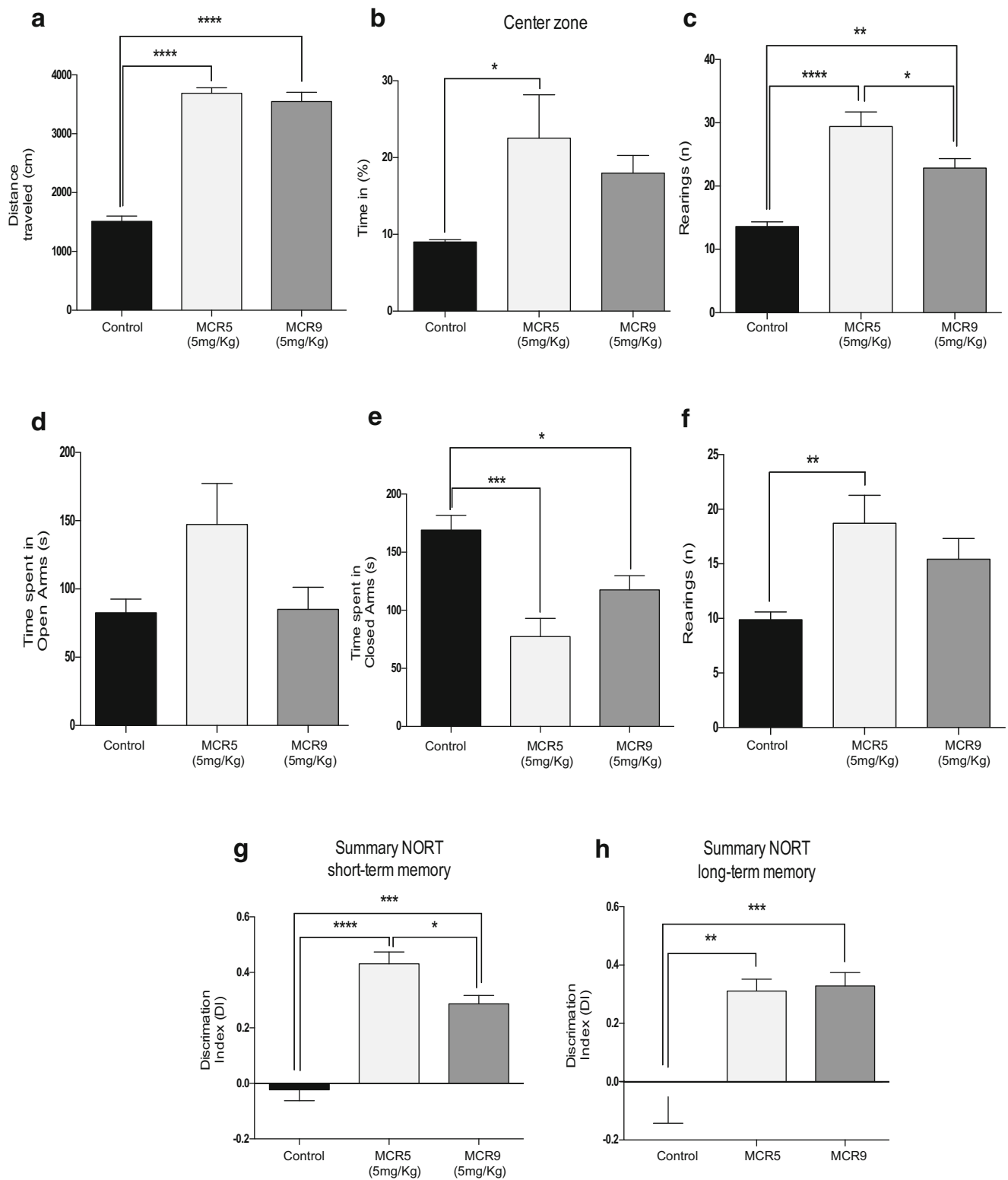


**Fig. 3.** Acute and repeated measurement of the hypothermic effect of compound **MCR9** in mice. **a** Effect of acute treatment with **MCR9** (20 mg/kg, i.p.) on rectal body temperature in mice. Columns are means  $\pm$  SEM of the difference ( $\Delta$ , 1 h - basal value) in body temperature ( $^\circ\text{C}$ ) for **MCR9**-treated mice compared with vehicle-treated **Control** mice. Data were analyzed using Student's *t*-test. \*\* $p < 0.01$ . **b** Effect of repeated (5

days) treatments with **MCR9** (20 mg/kg, i.p., closed circles) on rectal body temperature in mice. Circles are means  $\pm$  SEM of the difference ( $\Delta$ , 1 h - basal value) in body temperature ( $^\circ\text{C}$ ) for **MCR9**-treated mice compared with vehicle-treated **Controls**. Data were analyzed using repeated measures ANOVA followed by Sidak's multiple comparison test. \*\* $p < 0.01$ , \*\*\* $p < 0.001$ ; ( $n=6-7$  animals per group)



### Open Field (OFT), Elevated Plus Maze (EPM), and Novel Object Recognition Test (NORT)

The OFT apparatus was a white polywood box (50x50x25 cm). The floor was divided into two areas defined as center

zone and peripheral zone (15 cm between the center zone and the wall). Behavior was scored with SMART® vers. 3.0 software, and each trial was recorded for later analysis using a camera situated above the apparatus. Twenty-six mice (n=8-10 per group) were placed at the center and allowed to explore

◀ **Fig. 4.** Behavioral and cognitive improvement in 12-month-old treated SAMP8 mice with both I<sub>2</sub>-IR ligands. **a** A significant increase in the distance traveled in the open field test in the I<sub>2</sub>-IR ligand treated groups compared with the **Control** group. **b** A significant increase in the percentage of time in the center zone of the opened field test in the **MCR5** treated group compared with the **Control** group, and no significant difference between the **MCR9** and **Control** groups. **c** A significant increase in the number of total rears of the opened field test among groups. **d** The time spent in the opened arms of the EPM did not differ among groups. **e** A significant increase in the time spent in the closed arms among the **Control** group compared with the treated groups. **f** A significant increase in the number of total rears of the EPM in the **MCR5** group compared with the **Control** group. **g** The results of the NORT in the short-term memory (2 h) revealed a significant increase in both I<sub>2</sub>-IR ligand treated groups compared with the **Control** group as well as a significant reduction in the DI of the **MCR9** group compared with **MCR5** group, and **(h)** a significant increase in the DI of the long-term memory (24 h) in both I<sub>2</sub>-IR ligand treated groups compared with the **Control** group. Data expressed as means ± SEM (n=8-10 animals per group) and analyzed using one-way ANOVA followed by Tukey's post hoc test for multiple comparisons. \**p*<0.05, \*\**p*<0.01, \*\*\**p*<0.001 and \*\*\*\**p*<0.0001

the box for 5 min. Afterward, the mice were returned to their home cages and the OFT apparatus was cleaned with 70% EtOH. The parameters scored included center staying duration, rears, defecations, and the distance traveled, calculated as the sum of total distance traveled in 5 min.

The EMP apparatus consists of opened arms and closed arms, crossed in the middle perpendicularly to each other, and a central platform (5×5cm) constructed of dark and white plywood (30×5×15 cm). To initiate the test session, 26 mice (n=8-10 per group) were placed on the central platform, facing an open arm, and allowed to explore the apparatus for 5 min. After the 5-min test, mice were returned to their home cages, and the EPM apparatus was cleaned with 70% EtOH and allowed to dry between tests. Behavior was scored with SMART® vers. 3.0 software, and each trial was recorded for later analysis using a camera fixed to the ceiling at a height of 2.1 m and situated above the apparatus. The parameters recorded included time spent on opened arms, time spent on closed arms, time spent in the center zone, rears, defecation and urination.

The NORT protocol employed was a modification of that of Ennaceur and Delacour [39]. In brief, 26 mice (n=8-10 per group) were placed in a 90°, two-arm, 25-cm-long, 20-cm-high, 5-cm-wide black maze. The walls could be removed for easy cleaning. Light intensity in mid-field was 30 lux. Before performing the test, the mice were individually habituated to the apparatus for 10 min for 3 days. On day 4, the animals were submitted to a 10-min acquisition trial (first trial), during which they were placed in the maze in the presence of two identical, novel objects (A+A or B+B) at the end of each arm. A 10-min retention trial (second trial) was carried out 2 h and 24 h later, with one of the two objects changed. During these second trials, mice behavior was recorded with a camera. The time with the new object (TN) and the time with the old object (TO) were measured. A discrimination index (DI) was defined as (TN

−TO)/(TN+TO). The maze and the objects were cleaned with 96% EtOH after each test to eliminate olfactory cues.

## Brain Processing

Mice were euthanized by cervical dislocation 1 day after the behavioral and cognitive tests finished. Brains were immediately removed from the skull. The hippocampus of each mouse was then isolated and frozen in powdered dry ice. Each hippocampus was maintained at -80°C for further use. Tissue samples were homogenized in lysis buffer containing phosphatase and protease inhibitors (Cocktail II, Sigma-Aldrich). Total protein levels were obtained and the Bradford method was used to determine protein concentration.

## Protein Levels Determination by Western Blot (WB)

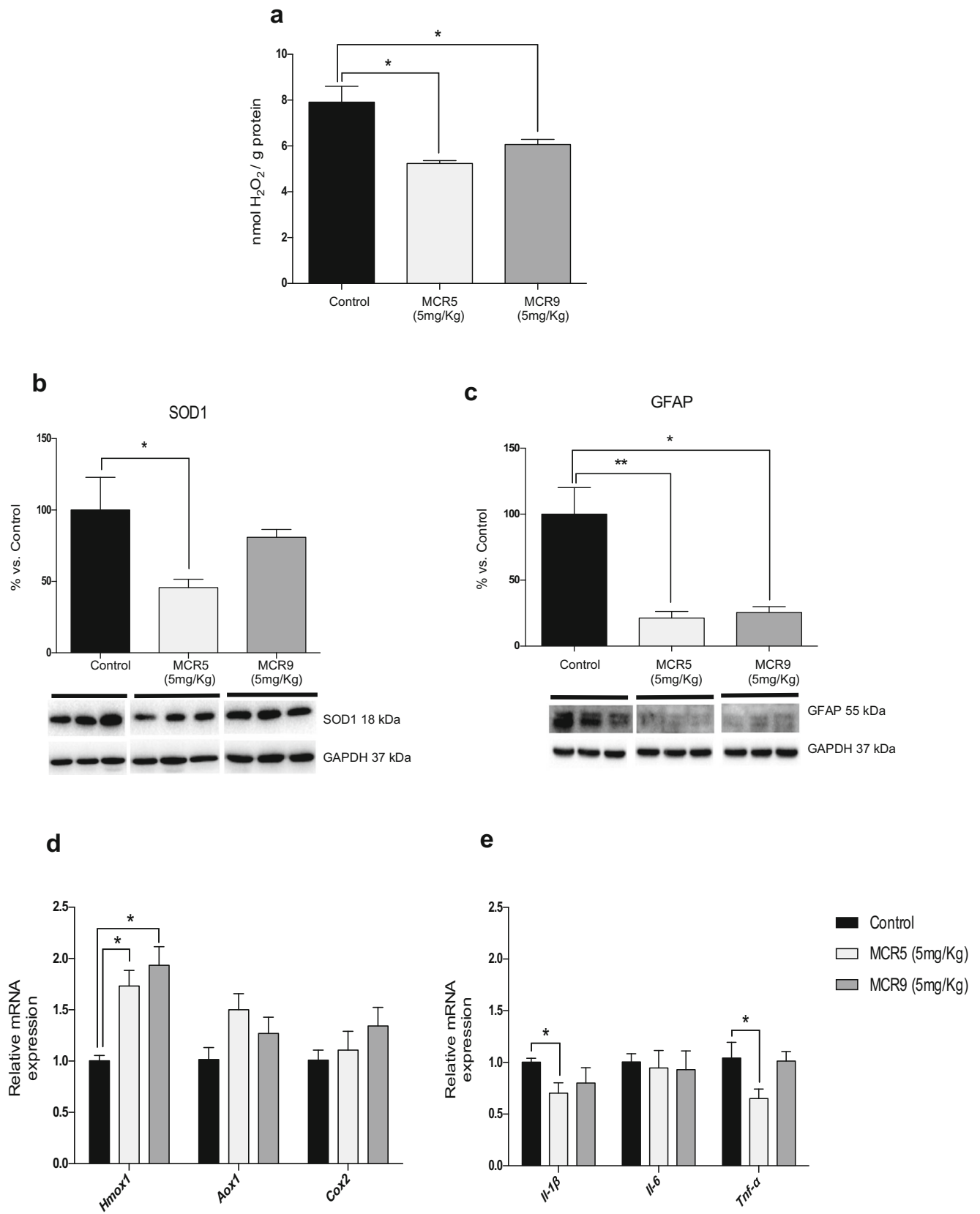
For WB, aliquots of 15 µg of hippocampal protein were used. Protein samples from 15 mice (n=5 per group) were separated by SDS-PAGE (8-12%) and transferred onto PVDF membranes (Millipore). Afterward, membranes were blocked in 5% non-fat milk in 0.1% Tween20 TBS (TBS-T) for 1 h at room temperature, followed by overnight incubation at 4°C with the primary antibodies listed in Table 1 (Supporting Information). Membranes were washed and incubated with secondary antibodies for 1 h at room temperature. Immunoreactive proteins were viewed with a chemiluminescence-based detection kit, following the manufacturer's protocol (ECL Kit; Millipore) and digital images were acquired using a ChemiDoc XRS+ System (BioRad). Semi-quantitative analyses were carried out using ImageLab software (BioRad), and results were expressed in arbitrary units, considering control protein levels as 100%. Protein loading was routinely monitored by immunodetection of glyceraldehyde-3-phosphate dehydrogenase (GAPDH).

## Determination of OS in the Hippocampus

Hydrogen peroxide (H<sub>2</sub>O<sub>2</sub>) from 12 mice (n=4 per group) was measured in hippocampal tissue protein extracts obtained as described above. It was used as an indicator of OS and was quantified using a hydrogen peroxide assay kit (Sigma-Aldrich, St. Louis, MI) according to the manufacturer's instructions.

## RNA Extraction and Gene Expression Determination

Total RNA isolation was carried out using the TRIzol® reagent according to manufacturer's instructions. The yield, purity, and quality of RNA were determined spectrophotometrically with a NanoDrop™ ND-1000 (Thermo Scientific) apparatus and an Agilent 2100B Bioanalyzer (Agilent Technologies). RNAs with 260/280 ratios and RIN higher than 1.9 and 7.5, respectively, were selected. Reverse Transcription-Polymerase Chain Reaction (RT-PCR) was



◀ **Fig. 5.** Reduced OS and inflammatory markers in 12-month-old treated SAMP8 mice with both I<sub>2</sub>-IR ligands. **a** There was a significant reduction in the hydrogen peroxide concentration in both I<sub>2</sub>-IR ligand treated groups compared with the **Control** group in homogenates of the hippocampus tissue. **b** A significant reduction in SOD1 protein levels in the **MCR5** group compared with the **Control** group and no difference between the **MCR9** and **Control** groups. **c** A significant reduction in *Gfap* protein levels in the **MCR5** and **MCR9** groups compared with the **Control** group. **d** Gene expression of antioxidant enzymes in the mouse hippocampus. A significant increase in *Hmox1* gene expression, but not for *Aox1* and *Cox2*, among both I<sub>2</sub>-IR ligand treated groups and the **Control** group. **e** A significant reduction in gene expression of *Il-1β* and *Tnf-α* in the **MCR5** group compared with the **Control** group, and a tendency for the same genes to reduce in the **MCR9** group. However, *Il-6* gene expression did not differ among groups. Values in bar graphs are adjusted to 100% for protein level of the **Control** group. Gene expression levels were determined by real-time PCR. Data are expressed as means ± SEM (n=4-5 animals per group) and analyzed using one-way ANOVA followed by Tukey's post hoc test for multiple comparisons. \**p*<0.05

performed as follows: 2 µg of mRNA was reverse-transcribed using the high capacity cDNA reverse transcription kit (Applied Biosystems). Real-time quantitative PCR (qPCR) was employed to quantify the mRNA expression of OS genes heme oxygenase (decycling) 1 (*Hmox1*), aldehyde oxidase 1 (*Aox1*), cyclooxygenase 2 (*Cox2*), inflammatory genes interleukin 6 (*Il-6*), interleukin 1 beta (*Il-1β*), tumor necrosis factor alpha (*Tnf-α*), amyloid processing gene disintegrin, and metalloproteinase domain-containing protein 10 (*Adam10*) and amyloid degradation gene neprilysin (*NEP*). The primers are listed in Table 2 (Supporting Information).

SYBR® Green real-time PCR was performed in a Step One Plus Detection System (Applied-Biosystems) employing SYBR® Green PCR Master Mix (Applied-Biosystems). Each reaction mixture contained 7.5 µL of cDNA (a 2-µg concentration), 0.75 µL of each primer (a 100-nM concentration, each), and 7.5 µL of SYBR® Green PCR Master Mix (2X).

TaqMan-based real-time PCR (Applied Biosystems) was also performed in a Step One Plus Detection System (Applied-Biosystems). Each 20 µL of TaqMan reaction contained 9 µL of cDNA (25 ng), 1 µL 20X probe of TaqMan Gene Expression Assays and 10 µL of 2X TaqMan Universal PCR Master Mix.

Data were analyzed using the comparative cycle threshold (Ct) method ( $\Delta\Delta Ct$ ), where the housekeeping gene level was used to normalize differences in sample loading and preparation. Normalization of expression levels was performed with *actin* for SYBR® green-based real-time PCR results and *Tbp* for TaqMan-based real-time PCR. Each sample (n=4-5 per group) was analyzed in duplicate, and the results represent the n-fold difference of the transcript levels among different groups.

### Statistical Analysis

The statistical analyses were conducted using GraphPad Prism ver. 6 statistical software. Data were expressed as the mean ±

standard error of the mean (SEM). Means were compared with one-way analysis of variance (ANOVA) and Tukey's post hoc test or two-tailed Student's *t*-test when necessary. Statistical significance was considered when *p* values were <0.05. Statistical outliers were performed out with Grubbs' test and were removed from the analysis.

## Results

### BBB Permeation Assay for I<sub>2</sub>-IR Ligands MCR5 and MCR9

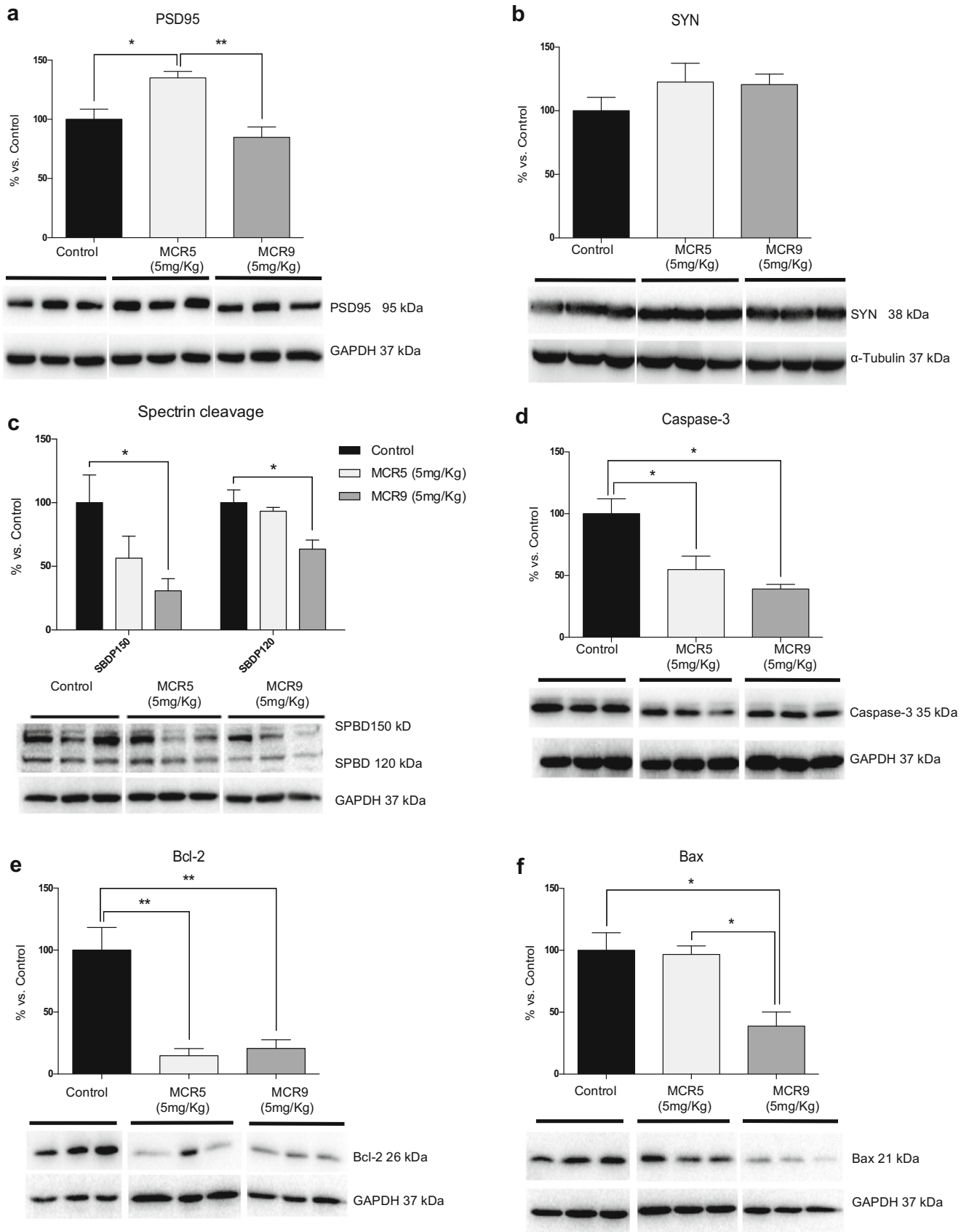
The tested compounds **MCR5** and **MCR9** had Pe values of 13.5±0.9 and 26.9±1.7, respectively, well above the threshold for high BBB permeation, so they were predicted to be able to cross the BBB and reach their biological target in the CNS. Supplementary information on results analysis can be found in the supporting material (Table 3).

### Hypothermic Effects of MCR9 in Mice

Selective I<sub>2</sub>-IR ligands induce hypothermia in rodents [4]. In particular, the hypothermic effect of compound **MCR5** in mice was evaluated in a recent study from our research group (results for compound **2c** in ref 35) [35]. Similar to **MCR5**, **MCR9** induced mild hypothermia as assessed by a moderate reduction (-2.3°C) in rectal temperature 1 h after injection at the tested dose of 20 mg/kg in adult CD-1 mice and as compared with vehicle-treated controls (Fig. 3a, day 1). While repeated (5 days) administration (20 mg/kg) revealed persistently the hypothermic effects of **MCR9** from days 1 to 4 (range from -2.3 to -3.2°C), on day 5 no significant change was observed in body temperature (-1.8°C change) as compared with vehicle-treated controls (Fig. 3b).

### Beneficial Effects on Behavior and Cognition Induced by MCR5 and MCR9 in SAMP8 Mice

Results obtained in OFT demonstrated that both compounds increased locomotor activity and time spent in the center zone (Fig. 4a and b). Furthermore, a significant increment in the vertical activity, quantified by the number of total rears, was observed in mice treated with **MCR5** or **MCR9** in OFT and the EPM (Fig. 4c and f). EPM data indicated a reduction in anxiety-like behavior by a significant decrease in time spent in closed arms for treated animals compared with controls (Fig. 4e). These results are supported by a preference for opened arms, although not significant, for **MCR5** (Fig. 4d). Moreover, a significant increase in the DI indicates an improved performance in recognition of the new object in the NORT between **MCR5**- and **MCR9**-treated SAMP8 mice compared with the control group. A robust effect in short (2





◀ **Fig. 6.** Changes in synaptic markers and apoptotic factors in 12-month-old treated SAMP8 mice with both I<sub>2</sub>-IR ligands. **a** A significant increase in PSD95 protein levels in the **MCR5** group compared with the other two groups. **b** A tendency for SYN protein levels to increase in both I<sub>2</sub>-IR ligand treated groups compared with the **Control** group. **c** A tendency for a reduction in the spectrin fragment SPBD 150, and a significant reduction in the spectrin fragment SPBD 120 in the **MCR9** group compared with the **Control** group. **d** A significant reduction in Caspase-3 protein levels in both I<sub>2</sub>-IR ligand groups compared with the **Control** group. **e** A significant reduction in Bcl-2 protein levels in both I<sub>2</sub>-IR ligand groups compared with the **Control** group. **f** A significant reduction in Bax protein levels in the **MCR9** group compared with the other groups. Values in bar graphs are adjusted to 100% for protein level of the **Control** group. Representative WB for each protein in the mouse hippocampus is shown. Data are expressed as means ± SEM (n=5 animals per group) and analyzed using one-way ANOVA followed by Tukey's post hoc test for multiple comparisons. \**p*<0.05, \*\**p*<0.001

h) and long-term (24 h) memory was found for the two tested compounds (Fig. 4g and h).

### OS and Inflammatory Markers Reduced by MCR5 and MCR9 in SAMP8 Mice

OS and neuroinflammation are thought to be key risk factors in the development of neurodegeneration. The hydrogen peroxide levels in the hippocampus were significantly reduced in brains of mice treated with either **MCR5** or **MCR9** compared with the control group (Fig. 5a). Of note, superoxide dismutase 1 (SOD1) protein levels in treated mice were reduced by **MCR5** but not by **MCR9** (Fig. 5b). Moreover, *Hmox1* gene expression, an important key enzyme in cellular antioxidant-defense, was also significantly increased with both **MCR5** and **MCR9** (Fig. 5d). Other OS markers, such as *Aox1* or *Cox2*, were not significantly altered (Fig. 5d). Regarding the inflammation markers, no changes were observed in *Il-6* gene expression for tested compounds, but a significant decrease in *Il-1β* and *Tnf-α* for **MCR5** treated SAMP8 mice was found (Fig. 5e). Moreover, a significant diminution in *Gfap* gene expression was determined, reinforcing the prevention of inflammatory processes by **MCR5** and **MCR9** (Fig. 5c).

### Changes in Synaptic Markers and Apoptotic Factors Induced by MCR5 and MCR9 in SAMP8 Mice

**MCR5**, but not **MCR9**, induced an increase in postsynaptic density protein 95 (PSD95) protein levels (Fig. 6a). Protein levels for synaptophysin (SYN), a presynaptic protein, showed a slight increase for both compounds, although it did not reach significance (Fig. 6b). To determine the implication of proteolytic processes in the **MCR5** and **MCR9** compounds, we found reduced levels of calpain (data not shown) with a significant diminution in 150 α-spectrin breakdown fragment (SPBD) (Fig. 6c). Furthermore, **MCR9** and

**MCR5** reduced caspase-3 activity in SAMP8 mouse hippocampi, because of the diminution of caspase-3 protein levels and 120 SPBD fragments, which reached significance for **MCR9** (Fig. 6c and d). Moreover, B-cell lymphoma 2 (Bcl-2) levels were diminished, and Bcl-2-associated X (Bax), a key protein in the apoptotic cascade, was reduced by **MCR5** (Fig. 6e and f), supporting a possible implication of I<sub>2</sub>-IR in apoptosis processes.

### Changes in Mitogen-Activated Protein Kinase (MAPK) Signaling Pathways Reduced Hyperphosphorylation of Tau Induced by MCR5 and MCR9 in SAMP8 Mice

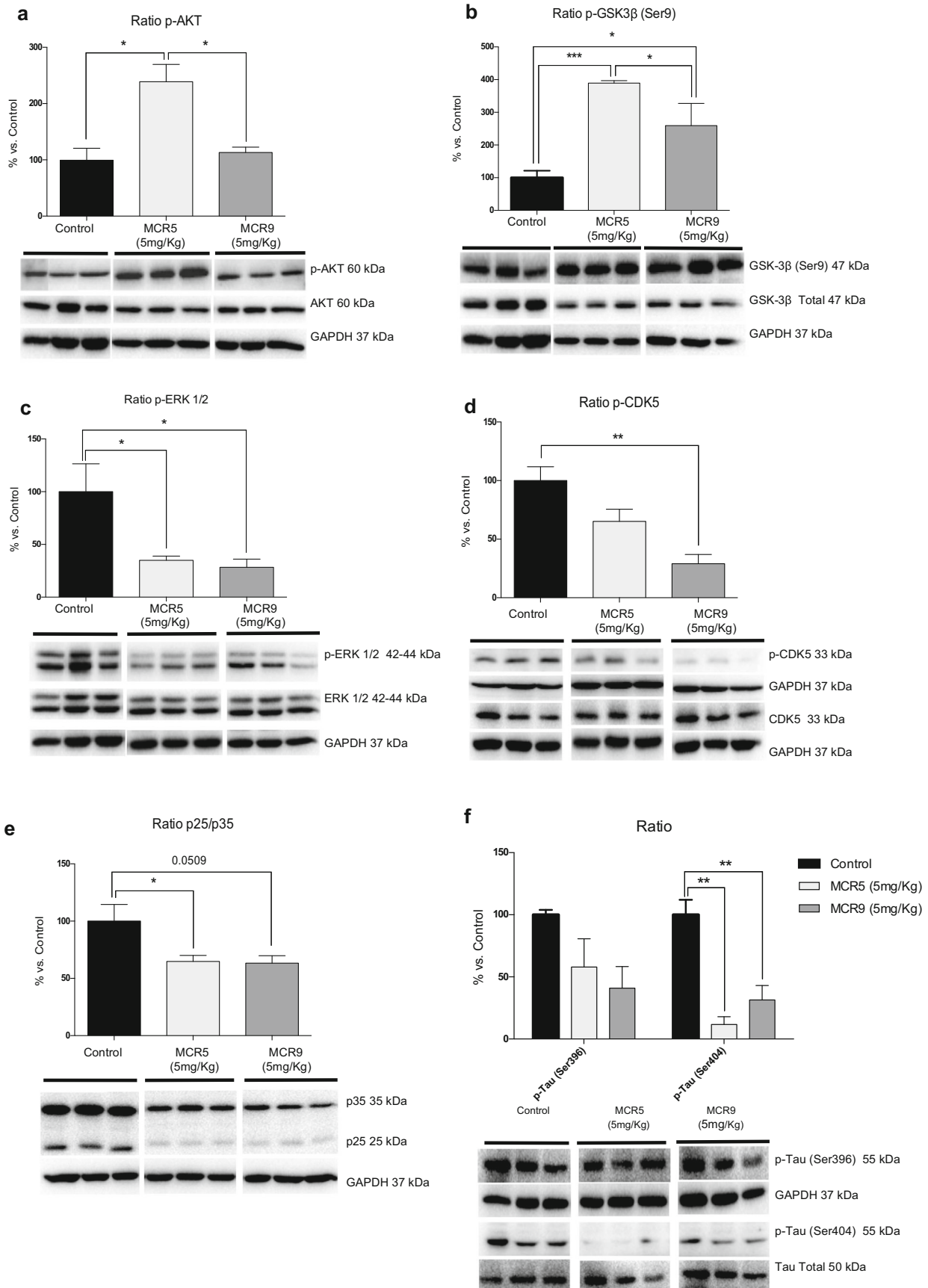
Key proteins associated with molecular pathways disturbed in brain disorders and neurodegeneration were evaluated by WB. Interestingly, **MCR5**, but not **MCR9**, increased the p-AKT/AKT ratio (protein kinase B) (Fig. 7a). Accordingly, higher levels of inactivated glycogen synthase kinase 3 beta (GSK3β), phosphorylated in Ser9, were determined (Fig. 7b). Extracellular signal-regulated kinase (ERK½) inhibition by **MCR5** and **MCR9** was demonstrated by a reduction of the p-ERK½ ratio (Fig. 7c). Furthermore, cyclin-dependent kinases 5 (CDK5) measured by the p-CDK5/CDK5 and p25/p35 ratios were also reduced (Fig. 7d and e). Taking into account the results obtained on kinases CDK5, GSK3β, AKT, and ERK½, we studied Tau hyperphosphorylation levels in the hippocampi of SAMP8 mice. A significant reduction in Tau phosphorylation in treated SAMP8 mice was found, specifically for the Ser404 phosphorylation site, whereas the Ser396 phosphorylation site was reduced without reaching significance (Fig. 7f).

### Changes in APP Processing and Aβ Degradation Induced by MCR5 and MCR9 in SAMP8 Mice

We found a significant increase in sAPPα protein levels in **MCR9** treated SAMP8 mice (Fig. 8a) and a significant reduction in sAPPβ protein levels in **MCR5** treated SAMP8 mice (Fig. 8b). Furthermore, a significant increase in gene expression for *Adam10*, an α-secretase that cleaves APP and *NEP*, an Aβ degrading enzyme (Fig. 8c and d), was observed in both treated mice groups compared with that in non-treated animals.

## Discussion

I<sub>2</sub>-IR are related to several physiological and pathological processes, including those of the CNS, such as pain [8], neuropathic pain [40], seizures [41, 42], and neurodegenerative diseases such as AD [14, 43]. Our lab has a research line on developing new high affinity and selectivity I<sub>2</sub>-IR ligands, maintaining the imidazoline scaffold and incorporating



◀ **Fig. 7.** Changes in kinase signaling pathways reduced hyperphosphorylation of Tau in 12-month-old SAMP8 mice treated with both I<sub>2</sub>-IR ligands. **a** A significant increase in the p-AKT ratio in the **MCR5** group compared with the other two groups. **b** A significant increase in inactive p-GSK3β (Ser9) protein levels in both I<sub>2</sub>-IR ligand treated groups compared with the **Control** group. **c** A significant reduction in p-ERK½ in both I<sub>2</sub>-IR ligand treated groups compared with the **Control** group. **d** Changes in the p-CDK5/CDK5 ratio induced by **MCR5** and **MCR9** treatment. **e** Changes in the p25/p35 ratio in the **MCR5** and **MCR9** groups compared with the **Control** group. Representative WB are shown. **f** A reduction in p-Tau (Ser396), as well as a significant reduction in p-tau (Ser404) in both I<sub>2</sub>-IR ligand treated groups compared with the **Control** group. Values in bar graphs are adjusted to 100% for protein level of the **Control** group. Data are expressed as means ± SEM (n=5 animals per group) and analyzed using one-way ANOVA followed by Tukey's post hoc test for multiple comparisons. \**p*<0.05, \*\**p*<0.01, \*\*\**p*<0.001

several substituents in the imidazoline ring. Some of these were previously tested for their neuroprotective role [35].

Given the enormous potential of I<sub>2</sub>-IR and their implications in brain disorders and neurodegenerative diseases such as AD, we set out to explore whether **MCR5** and **MCR9**, two members of a structurally new family of I<sub>2</sub>-IR ligands, might improve the behavioral and cognitive status in SAMP8 model mice. The main chemical structural differences were a phosphonate substituent on the imidazoline ring for **MCR5** in contrast with an ester group for **MCR9** (Fig. 2).

Published results from our lab demonstrated that **MCR5** presented a pKi for the I<sub>2</sub>-IR of 9.42±0.16 and high selectivity when compared with the α<sub>2</sub> receptor affinity [35]. Likewise, **MCR9** is a high-affinity I<sub>2</sub>-IR ligand (pKi 8.85±0.21) but with a higher selectivity against α<sub>2</sub> receptors. Both **MCR5** and **MCR9** were predicted to be able to cross the BBB, an important drug characteristic when action is expected in the CNS.

Previous studies have evaluated the effects of selective I<sub>2</sub>-IR ligands on inducing hypothermia in rodents [e.g., idazoxan or BU224] [44]. Accordingly, **MCR5** can induce hypothermia in mice, and showed a neuroprotective role in kainate-induced seizures, modifying levels of a Fas-associated protein with death domain (FADD) receptor [35]. While acute **MCR5** (5 and 20 mg/kg) induced mild hypothermia, repeated (20 mg/kg, 5 days) administration of **MCR5** revealed significantly attenuated hypothermic effects from day 2, which indicated the induction of tolerance to the hypothermic effects of the drug [35]. For **MCR9**, repeated (20 mg/kg, 5 days) administration revealed persistent hypothermic effects up to day 4. These results suggest that the slow induction of tolerance to the hypothermic effects caused by **MCR9** might be started following 5 days of drug administration, although a more extended treatment paradigm might be needed for confirmation.

The hypothermic effects exerted by **MCR5** and **MCR9** might be relevant to induce neuroprotection because it was

previously proposed for some of the neuroprotective effects induced by the I<sub>2</sub>-IR selective ligand idazoxan. Several experiments have ascertained a possible role for hypothermia in mediating neuroprotection. For example, small drops in temperature exerted neuroprotection in cerebral ischemia [45] and are typically used in the clinic to improve the neurological outcome under various pathological conditions (e.g., stroke, brain injury). Although the mechanisms explaining the neuroprotective effects mediated by hypothermia are not well understood, some researchers have suggested that they might be related to the inhibition of glutamate release [46].

SAMP8 mice have been studied as a non-transgenic murine mouse model of accelerated senescence and late-onset AD. These mice exhibit cognitive and emotional disturbances, probably due to the early development of pathological brain hallmarks, such as OS, inflammation, and activation of neuronal death pathways, which mainly affect the cerebral cortex and hippocampus [47, 48]. To date, this rodent model has not been used to test I<sub>2</sub>-IR ligands. Thus, this work is the first investigation of the effects of the improvement of cognitive impairment and behavior in this mouse model after treatment with I<sub>2</sub>-IR ligands.

Behavioral and cognitive effects were investigated through three well-established tests in SAMP8 mice: the OFT, which is an experiment used to assay general locomotor activity and anxiety in rodents [49]; the EPM, one of the most widely used tests for measuring anxiety-like behavior [50]; and the NORT, as a standard measure of cognition (for short- and long-term memory) [51].

The OFT and EPM parameters indicated a reduction in cognitive impairment through showing improved locomotor activity jointly with an anti-anxiousness effect. Likewise, the NORT results demonstrated an improvement in cognitive and short- and long-term learning capabilities in hippocampal memory processes. Therefore, all the assessed parameters showed robust beneficial effects on cognition and behavior after **MCR5** and **MCR9** treatment in SAMP8 mice.

The results in cognitive and behavioral effects were supported by a cellular and biochemical assessment of characteristic parameters related to cognitive decline and AD. The compelling evidence demonstrated a neuroprotective role for I<sub>2</sub>-IR. The neuroprotective role can be related to OS and inflammation [52] by measuring OS indicators and inflammation markers in SAMP8 mouse brain tissue treated with the I<sub>2</sub>-IR ligands, **MCR5** and **MCR9**. Results showed significant reduced hydrogen peroxide levels in hippocampal tissue and increased *Hmox1* gene expression in treated **MCR5** and **MCR9** SAMP8 mice, but not in other sensors for OS, such as *Aox1* or *Cox2*. SOD1 protein levels were reduced by **MCR5** but not by **MCR9**. Regarding inflammation markers, no changes were observed in *Il-6* gene expression for tested compounds, but a significant decrease in *Il-1β* and *Tnf-α* for **MCR5** treated SAMP8 mice was

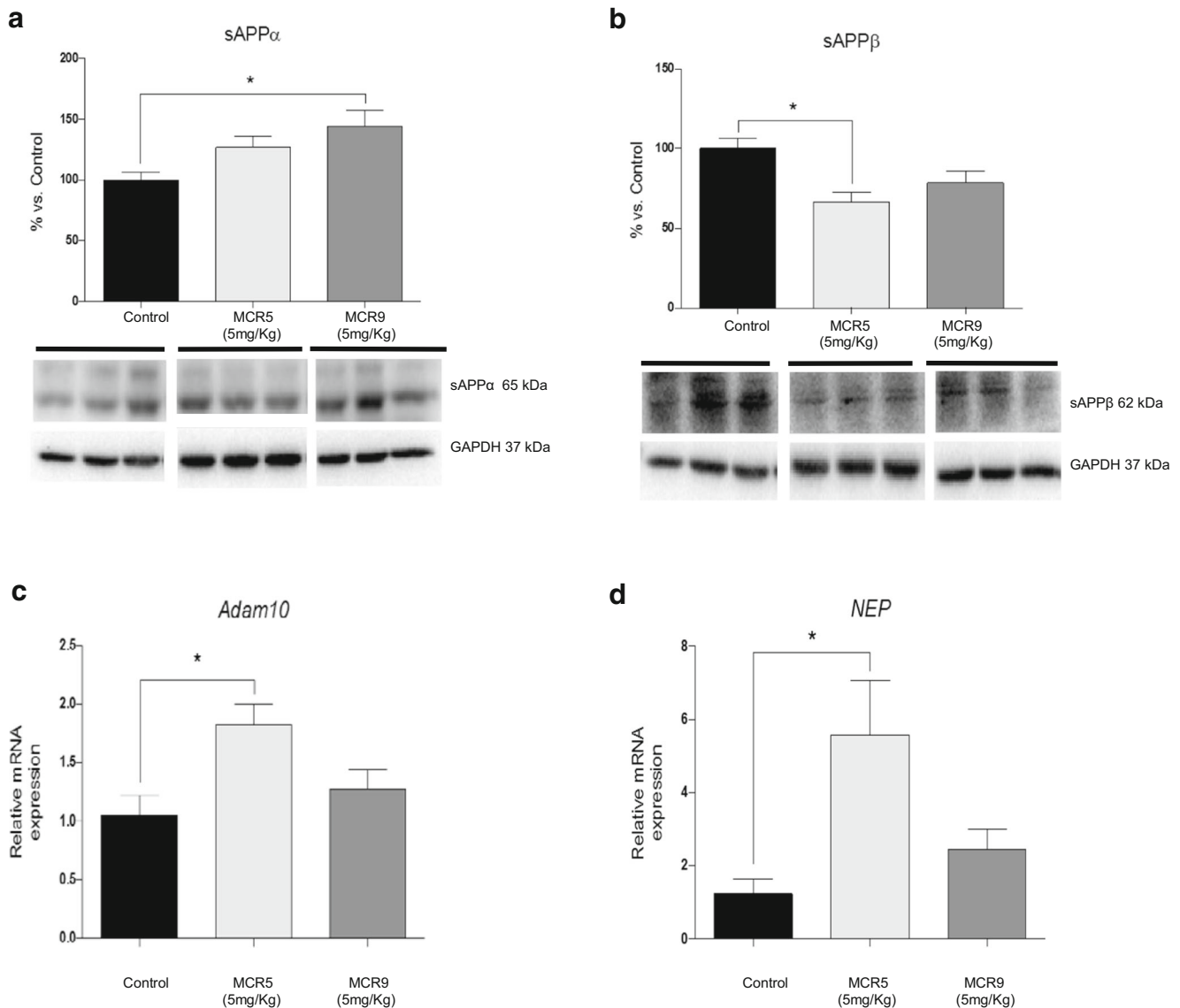


**Fig. 8.** Changes in APP processing and A $\beta$  degradation enzymes in 12-month-old SAMP8 mice treated with both I<sub>2</sub>-IR ligands. Representative WB of the APP and its fragments. **a** A significant increase in sAPP $\alpha$  protein levels in the **MCR9** group compared with the **Control** group, and no significant difference between the **MCR5** and **Control** groups. **b** A significant reduction in sAPP $\beta$  protein levels in the **MCR5** group compared with the **Control** group, and no significant difference between the **MCR9** and **Control** groups. **c** A significant increase in *Adam10* gene expression in the **MCR5** group compared with the **Control** group, and no

significant difference in the **MCR9** group. **d** A significant increase in *NEP* gene expression in the **MCR5** group compared with the **Control** group, and no significant difference in the **MCR9** group. Values in bar graphs were adjusted to 100% for protein level of the **Control** group. Gene expression levels were determined by real-time PCR. Data are expressed as means  $\pm$  SEM (n=4-5 animals per group) and analyzed using one-way ANOVA followed by Tukey's post hoc test for multiple comparisons. \* $p$ <0.05

found. In addition, reduced astrogliosis was found in treated animals, corroborating a reduced inflammatory environment in hippocampi of **MCR5** and **MCR9** treated SAMP8 mice. Altogether these results showed a relatively weak influence in OS and inflammation mechanisms by I<sub>2</sub>-IR ligands in SAMP8 mice [53–57]. However, a role for those two pathological conditions related to I<sub>2</sub>-IR ligand interaction cannot be discarded because **MCR5** elicited beneficial effects despite the old age of the SAMP8 mice. Aged SAMP8 mice present lower inflammation and OS due to

being at the endpoint of the senescence process [56, 57]. Therefore, it can be challenging to determine drug effects on these processes in aged SAMP8 mice.

**MCR5** and **MCR9** effects on key molecular markers for synapsis and apoptosis were studied to unravel the prevention of cognitive decline by I<sub>2</sub>-IR ligands in SAMP8 mice, which is characterized by alterations in those processes. In consonance with better cognitive performance, the compounds tested increased synaptic markers such as SYN and PSD95, indicating a neuroprotective role for **MCR5** and **MCR9**.

There are several cellular and molecular pathways related to better synaptic performance, including proteolytic and phosphorylation activities or apoptotic processes. Regarding proteolytic processes, calpain is an intracellular protease that cleaves the CDK5 activator p35 to a p25 fragment. **MCR5** and **MCR9** diminished calpain levels and its activity with a reduced 150 SPBD fragment. Moreover, a significant reduction in p25 protein levels was found in treated SAMP8 mice. A decrease in p25 can also influence CDK5 activity, as implicated in Tau phosphorylation [58, 59]. These results indicate that CDK5 phosphorylation activity should be diminished after I<sub>2</sub>-IR ligand treatment, corroborating results obtained previously for **MCR5** in a kainate model of neuronal damage [60].

Caspase 3 mediated apoptosis was also addressed. A significant reduction of caspase 3 activity and diminution of Bax protein were found in **MCR9** treated SAMP8 mice. Because Bax is described as a pro-apoptotic protein, its diminution indicates a possible protective role for I<sub>2</sub>-IR ligands in neurons [61]. By contrast, reduced levels of Bcl-2, considered an anti-apoptotic protein, deserve further studies. Several authors have indicated that when Bax is reduced, Bcl-2 is less necessary for blocking Bax dimer to form the mitochondrial pore; in this situation cells reduce the Bcl-2 levels as a control mechanism [62].

An increase in p-AKT was induced by the I<sub>2</sub>-IR ligands, whereas a decrease in ERK $\frac{1}{2}$  activation was observed. p-AKT inactivated GSK3 $\beta$ , a key kinase involved in the process of Tau hyperphosphorylation, by phosphorylation in Ser9. To this point, **MCR5**- and **MCR9**-treated SAMP8 mice showed an increase of Ser9 phosphorylated GSK3 $\beta$  and reduced Tau hyperphosphorylation.

ERK $\frac{1}{2}$  inhibition (that reduction of p42/p44) by **MCR5** and **MCR9** can contribute to the beneficial effect elicited by I<sub>2</sub>-IR on synaptic markers and Tau phosphorylation processes. ERK $\frac{1}{2}$  belongs to a subfamily of MAPKs and plays diverse roles in the CNS, such as neuronal survival or death, synaptic plasticity, and learning and memory through phosphorylation of regulatory enzymes and kinases [63, 64]. Although crucial for neuronal survival, there is some evidence that prolonged activation of the ERK pathway can induce a deleterious effect to the cell [65, 66]. Interestingly, long-lasting ERK activation in neurons has been demonstrated in neurodegenerative diseases such as AD [67, 68] and PD [69]. Here, the inhibition of this kinase participates in post-translational modifications in cytoskeletal proteins such as Tau, ameliorating the neuronal network functioning, as demonstrated with an increase in synaptic markers.

The relationship among MAPKs, such as ERK $\frac{1}{2}$  [70], and PI3K, such as AKT, and imidazoline receptors is well defined [71, 72]. In this respect, it has been described that either ERK or AKT can be associated with the multifunctional *Fas/FADD* complex [73, 74]. Apoptosis is an important contributor to neurodegeneration [75], and in this regard, the FADD protein has been

suggested as a putative biomarker for pathological processes associated with the course of clinical dementia [76]. It has been reported that total FADD has a central role in promoting apoptosis [77, 78] and its phosphorylation at Ser191/194 mediates non-apoptotic actions such as cell growth and differentiation [79]. In our previous work, we demonstrated that **MCR5** modified FADD phosphorylation (i.e., it increased the p-FADD/FADD ratio) in a kainate-treated rat model [35]. These results could explain the modulation of proteins from the apoptotic pathway mentioned before (e.g., a diminution in caspase 3 activation and significant changes in Bcl-2 and Bax), which seems to favor anti-apoptotic actions mediated through I<sub>2</sub>-receptors, and especially by **MCR5**.

Tau hyperphosphorylation is a histological trend in many neurodegenerative diseases characterized by cognitive decline, including AD. Therefore, we studied APP processing pathways. Aberrant APP processing is a hallmark of cognitive decline diseases [80]. To assess the capacity of the tested compounds to modify this pathological hallmark, we evaluated APP fragments, specifically, sAPP $\alpha$  and sAPP $\beta$ . Despite neither APP fragment reaching significance in either I<sub>2</sub>-IR ligand-treated SAMP8 mice group, we found a clear tendency that indicates the non-amyloidogenic pathway preference. Moreover, sAPP $\alpha$  is described as a neuroprotective, neurotrophic and cell excitable regulator with synaptic plasticity [81]. *Adam10* [82] and *NEP* [83] gene expression were higher in **MCR5** and **MCR9** treated mice groups than in non-treated animals. In sum, I<sub>2</sub>-IR ligands foster a diminution in the amyloidogenic pathway and higher degradation of  $\beta$ -amyloid in the SAMP8 mice model.

In conclusion, the effectiveness of the two new I<sub>2</sub>-IR ligands in an *in vivo* female model for cognitive decline was demonstrated in this study. SAMP8 model mice are gated to neurodegenerative processes, such as AD, and our research has shown that **MCR5** and **MCR9** can open new therapeutic avenues against these pathological conditions that currently have unmet medical needs. Although different authors have previously indicated the relationship between I<sub>2</sub>-IR and cognitive decline, this study is the first experimental evidence that demonstrates the possibility of using this receptor as a target for cognitive impairment. Here, we demonstrate that this strategy could represent a future approach to treating devastating conditions such as AD.

**Acknowledgments** This study was supported by the Ministerio de Economía y Competitividad of Spain (SAF2016-77703 and SAF2014-55903-R) and the Basque Government (IT616/13). C.G.-F., F.V., F.X.S., C.E. and M.P. belong to 2017SGR106 (AGAUR, Catalonia). J.A.G.-S. is a member emeritus of the Institut d'Estudis Catalans (Barcelona, Catalonia). Financial support was provided for F.V. (University of Barcelona, APIF\_2017), S.R.-A. (Generalitat de Catalunya, 2018FI\_B\_00227) and A.B. (Institute of Biomedicine UB\_2018).

**Required Author Forms** Disclosure forms provided by the authors are available with the online version of this article.

**Author Contributions** C.G.-F. and F.V. contributed equally. C.G.-F., C.E., L.F.C. and M.P. designed the study. B.P. performed the PAMPA-BBB permeation experiments. C.G.-F. and F.V. carried out the behavior and cognition studies and cellular parameters determination (OS and inflammation markers, synaptic markers and apoptotic factors, and hyperphosphorylation of Tau). J.A.G.-S. and M.J.G.-F. performed the hypothermic studies. S.A., S.R.-A. and A.B. synthesized and purified the I<sub>2</sub>-IR ligands. C.G.-F., L.F.C., F.X.S., J.A.G.-S., M.J.G.-F., C.E. and M.P. contributed to writing the manuscript. All authors have read and approved the final version of the manuscript.

**Abbreviations** AD, Alzheimer's disease; *Adam10*, A disintegrin and metalloproteinase domain-containing protein 10; ANOVA, One-way analysis of variance; APP, Amyloid precursor protein; *Aox1*, Aldehyde oxidase 1; AKT, Protein kinase B; Bcl-2, B-cell lymphoma 2; Bax, Bcl-2-associated X; BBB, Blood-brain barrier; CDK5, Cyclin-dependent kinase 5; CNS, Central nervous system; *Cox2*, Cyclooxygenase 2; Ct, Cycle threshold; DI, Discrimination index; EPM, Elevated plus maze; ERK, Extracellular signal-regulated kinase; GAPDH, Glyceraldehyde-3-phosphate dehydrogenase; FADD, Fas-associated protein with death domain; *Gfap*, Glial fibrillary acidic protein; GSK3 $\beta$ , Glycogen synthase kinase 3 beta; *Hmox1*, Heme oxygenase (decycling) 1; I<sub>2</sub>-IR, I<sub>2</sub>-Imidazoline receptors; *Il-1 $\beta$* , Interleukin 1 beta; *Il-6*, Interleukin 6; MAO, Monoamine oxidases; MAPK, Mitogen-activated protein kinase; *NEP*, Nephrylin; NMDA, *N*-methyl-D-aspartate; NORT, Novel object recognition test; OFT, Open field test; OS, Oxidative stress; PCR, Polymerase chain reaction; PD, Parkinson's disease; Pe, Permeability; PI3K, Phosphatidylinositol-4,5-bisphosphate 3-kinase; PSD95, Postsynaptic density protein 95; SAMP8, Senescence accelerated mouse prone 8; SPBD, Spectrin breakdown; SEM, Standard error of the mean; SOD1, Superoxide dismutase 1; SYN, Synaptophysin; TBP, Tata-binding protein; TN, Time with new object; *Tnf- $\alpha$* , Tumor necrosis factor alpha; TO, Time with old object; WB, Western blot

## REFERENCES

- Bousquet P, Feldman J, Schwarts J. Central cardiovascular effects of alpha-adrenergic drugs: differences between catecholamines and imidazolines. *J. Pharmacol. Exp. Ther.* 1984;230:232-236.
- Head GA, Mayorov DN. Imidazoline receptors, novel agents and therapeutic potential. *Cardiovasc. Hematol Agents Med. Chem.* 2006;4:17-32.
- Lowry JA, Brown JT. Significance of the imidazoline receptors in toxicology. *Clin. Toxicol.* 2014;52:454-469.
- Li, JK. Imidazoline I<sub>2</sub> receptors: An update. *Pharmacol. Ther.* 2017;178:48-56.
- Fenton, C, Keating, G M, Lyseng-Williamson KA. Moxonidine: a review of its use in essential hypertension. *Drugs* 2006;6:477-496.
- Reid JL. Rilmenidine: A clinical overview. *Am. J. Hypertens.* 2000;13:106S-111S.
- Olmos G, Alemany R, Boronat MA, García-Sevilla JA. Pharmacologic and molecular discrimination of I<sub>2</sub>-imidazoline receptor subtypes. *Ann. N.Y. Acad. Sci.* 1999;881:144-160.
- Li JX, Zhang Y. Imidazoline I<sub>2</sub> receptors: target for new analgesics? *Eur. J. Pharmacol.* 2011;658:49-56.
- Callado LF, Martín-Gomez JI, Ruiz J, Garibi J, and Meana JJ. Imidazoline I<sub>2</sub> receptors density increases with the malignancy of human gliomas. *J. Neurol., Neurosurg. Psychiatry* 2004;75:785-787.
- Regunathan S, Feinstein DL, Reis DJ. Anti-proliferative and anti-inflammatory actions of imidazoline agents. Are imidazoline receptors involved? *Ann. N.Y. Acad. Sci.* 1999;881:410-419.
- Ruiz J, Martín I, Callado LF, Meana JJ, Barturen F, García-Sevilla JA. Non-adrenoreceptor [<sup>3</sup>H] idazoxan binding sites (I<sub>2</sub>-imidazoline sites) are increased in postmortem brain from patients with Alzheimer's disease. *Neurosci. Lett.* 1993;160:109-112.
- García-Sevilla JA, Escribá PV, Walzer C, Bouras C, Guimón J. Imidazoline receptor proteins in brains of patients with Alzheimer's disease. *Neurosci. Lett.* 1998;247:95-98.
- Gargalidis-Moudanos C, Pizzinat N, Javoy-Agud F, Remaury A, Parini A. I<sub>2</sub>-imidazoline binding sites and monoamine oxidase activity in human postmortem brain from patients with Parkinson's disease. *Neurochem. Int.* 1997;30:31-36.
- Meana JJ, Barturen, F, Martín I, García-Sevilla JA. Evidence of increased non-adrenoreceptor [<sup>3</sup>H]idazoxan binding sites in the frontal cortex of depressed suicide victims. *Biol. Psychiatry* 1993;34:498-501.
- García-Sevilla JA, Escribá PV, Sastre, et al. Immunodetection and quantitation of imidazoline receptor proteins in platelets of patients with major depression and in brains of suicide victims. *Arch. Gen. Psychiatry* 1996;53:803-810.
- Smith KL, Jessop DS, Finn DP. Modulation of stress by imidazoline binding sites: implications for psychiatric disorders. *Stress* 2009;12:97-114.
- Comi E, Lanza M, Ferrari F, Mauri V, Caselli G, Rovati LC. Efficacy of CR4056, a first-in-class imidazoline-2 analgesic drug, in comparison with naproxen in two rat models of osteoarthritis. *J. Pain Res.* 2017;10:1033-1043.
- Regunathan S, Reis DJ. Imidazoline receptors and their endogenous ligands. *Ann. Rev. Pharmacol. Toxicol.* 1996;36:511-544.
- Dardonville C, Rozas I. Imidazoline binding sites and their ligands: an overview of the different chemical structures. *Med. Res. Rev.* 2004;24:639-661.
- Boronat MA, Olmos G, García-Sevilla JA. Attenuation of tolerance to opioid-induced antinociception and protection against morphine-induced decrease of neurofilament proteins by idazoxan and other I<sub>2</sub>-imidazoline ligands. *Br. J. Pharmacol.* 1998;125:175-185.
- McDonald GR, Olivieri A, Ramsay RR, Holt A. On the formation and nature of the imidazoline I<sub>2</sub> binding site on human monoamine oxidase B. *Pharmacol. Res.* 2010;62:475-488.
- Casanovas A, Olmos G, Ribera J, Boronat MA, Esquerda JE, García-Sevilla JA. Induction of reactive astrocytosis and prevention of motoneuron cell death by the I<sub>2</sub>-imidazoline receptor ligand LSL 60101. *Br. J. Pharmacol.* 2000;130:1767-1776.
- Gustafson I, Westerberg E, Wieloch T. Protection against ischemia-induced neuronal damage by the  $\alpha_2$ -adrenoceptor antagonist idazoxan: influence of time of administration and possible mechanisms of action. *J. Cereb. Blood Flow Metab.* 1990;10:885-894.
- Qiu WW, Zheng RY. Neuroprotective effects of receptor imidazoline 2 and its endogenous ligand agmatine. *Neurosci. Bull.* 2006;22:187-191.
- Gilad GM, Gilad VH. Accelerated functional recovery and neuroprotection by agmatine after spinal cord ischemia in rats. *Neurosci. Lett.* 2000;296:97-100.
- Han Z, Xiao MJ, Shao B, Zheng RY, Yang GY, Jin K. Attenuation of ischemia induced rat brain injury by 2-(-2-benzofuranyl)-2-imidazoline, a high selectivity ligand for imidazoline I(2) receptors. *Neurol. Res.* 2009;31:390-395.
- Maiese K, Pek L, Berger SB, Reis D J. Reduction in focal cerebral ischemia by agents acting at imidazole receptors. *J. Cereb. Blood Flow Metab.* 1992;12:53-63.
- Jiang SX, Zheng RY, Zheng JQ, Li XL, Han Z, Hou ST. Reversible inhibition of intracellular calcium influx through NMDA receptors by imidazoline (I)2 receptor antagonists. *Eur. J. Pharmacol.* 2010;629:12-19.

29. Ruggiero DA, Regunathan S, Wang H, Milner TA, Reis DJ. Immunocytochemical localization of an imidazoline receptor protein in the central nervous system. *Brain Res.* 1998;780:270–293.
30. Olmos G, Alemany R, Escriba PV, García-Sevilla JA. The effects of chronic imidazoline drug treatment on glial fibrillary acidic protein concentrations in rat brain. *Br. J. Pharmacol.* 1994;111:997–1002.
31. Rodríguez-Arellano JJ, Parpura V, Zorec R, Verkhratsky, A. Astrocytes in physiological aging and Alzheimer's disease. *Neuroscience* 2016;323:170–182.
32. Martín-Gómez JJ, Ruíz J, Barrondo S, Callado, LF, Meana JJ. Opposite changes in Imidazoline I<sub>2</sub> receptors and  $\alpha_2$ -adrenoceptors density in rat frontal cortex after induced gliosis. *Life Sci.* 2005;78: 205–209.
33. Sica DA. Alpha 1-adrenergic blockers: current usage considerations. *J. Clin. Hypertens. (Greenwich)* 2005;7:757–762.
34. Abás S, Estarellas C, Luque FJ, Escolano C. Easy access to (2-imidazolin-4-yl)phosphonates by a microwave assisted multicomponent reaction. *Tetrahedron* 2015;71:2872–2881.
35. Abás S, Erdozain AM, Keller B et al. Neuroprotective effects of a structurally new family of high affinity imidazoline I<sub>2</sub> receptors ligands. *ACS Chem. Neurosci.* 2017;8:737–742.
36. Morley JE, Farr SA, Kumar VB, Armbrrecht HJ. The SAMP8 mouse: a model to develop therapeutic interventions for Alzheimer's disease. *Curr. Pharm. Des.* 2012;18:1123–1130.
37. Di L, Kerns EH, Fan K, McConnell OJ, Carter G. T. High throughput artificial membrane permeability assay for blood-brain barrier. *Eur. J. Med. Chem.* 2003;38:223–232.
38. McGrath JC, Lilley E. Implementing guidelines on reporting research using animals (ARRIVE etc.): new requirements for publication in *BJP. Br. J. Pharmacol.* 2015;172:3189–3193.
39. Ennaceur A, Delacour J. A new one-trial test for neurobiological studies of memory in rats. 1: Behavioral data. *Behav. Brain Res.* 1988;31:47–59.
40. Ferrari F, Fiorentino S, Mennuni L, Garofalo P, Letari O, Mandelli S, Giordani A, Lanza M, Caselli G. Analgesic efficacy of CR4056, a novel imidazoline-2 receptor ligand, in rat models of inflammatory and neuropathic pain. 2011;4:111–125.
41. Jackson HC, Ripley TL, Dickinson SL, Nutt DJ. Anticonvulsant activity of the imidazoline 6,7-benzodiazoxan. *Epilepsy Res.* 1991;9(2):121–126.
42. Min JW, Peng BW, He X, Zhang Y, Li JX. Gender difference in epileptogenic effects of 2-BFI and BU224 in mice. *Eur J Pharmacol.* 2013;718(1-3):81–86.
43. Keller B, García-Sevilla JA. Immunodetection and subcellular distribution of imidazoline receptor proteins with three antibodies in mouse and human brains: Effects of treatments with I1- and I2-imidazoline drugs. *J Psychopharmacol.* 2015;29(9):996–1012.
44. Thorn DA, An XF, Zhang Y, Pignini M, Li, JX. Characterization of the hypothermic effects of imidazoline I<sub>2</sub> receptor agonist in rats. *Br. J. Pharmacol.* 2009;166:1936–1945.
45. Craven JA, Conway EL. Effects of alpha 2-adrenoceptor antagonists and imidazoline 2-receptor ligands on neuronal damage in global ischemia in the rat. *Clin. Exp. Pharmacol. Physiol.* 1997;24:204–207.
46. Ilievich UM, Zornow MH, Choi KT, Scheller M, Strnat MA. Effects of hypothermic metabolic suppression on hippocampal glutamate concentrations after transient global cerebral ischemia. *Anesth. Analg.* 1994;78:905–911.
47. Takeda T. Senescence-accelerated mouse (SAM) with special references to neurodegeneration models, SAMP8 and SAMP10 mice. *Neurochem. Res.* 2009;34:639–659.
48. Pallàs M. Senescence-accelerated mice P8: a tool to study brain aging and Alzheimer's disease in a mouse model. *ISRN Cell Biol.* 2012:1–12.
49. Archer J. Tests for emotionality in rats and mice: A review. *Anim. Behav.* 1973;21:205–235.
50. Dawson GR, Tricklebank MD. Use of the elevated plus maze in the search for novel anxiolytic agents. *Trends Pharmacol. Sci.* 1995;16: 33–36.
51. Antunes M, Biala G. The novel object recognition memory: neurobiology, test procedure, and its modifications. *Cogn. Process.* 2012;13:93–110.
52. Gao H-M, Zhou H, Hong JS. Oxidative Stress, Neuroinflammation, and Neurodegeneration. In: Peterson P. K., Toborek M. (Eds) *Neuroinflammation and Neurodegeneration*, 2014; pp. 81–104, Springer, New York, NY.
53. Fujibayashi Y, Yamamoto S, Waki A, Konishi J, Yonekura Y. Increased mitochondrial DNA deletion in the brain of SAMP8, a mouse model for spontaneous oxidative stress brain. *Neurosci. Lett.* 1998;254:109–112.
54. Sureda FX, Gutierrez-Cuesta J, Romeu M, Mulero M, Canudas AM, Camins A, Mallol J, Pallàs M. Changes in oxidative stress parameters and neurodegeneration markers in the brain of the senescence-accelerated mice SAMP-8. *Exp. Gerontol.* 2006;41: 360–367.
55. Gutierrez-Cuesta J, Sureda FX, Romeu M, Canudas AM, Caballero B, Coto-Montes A, Camins A, Pallàs M. Chronic administration of melatonin reduces cerebral injury biomarkers in SAMP8. *J. Pineal Res.* 2007;42:394–402.
56. Griñán-Ferré C, Palomera-Avalos V, Puigoriol-Illamola D, Camins A, Porquet D, Plà V, Aguado F, Pallàs M. Behaviour and cognitive changes correlated with hippocampal neuroinflammation and neuronal markers in SAMP8, a model of accelerated senescence. *Exp. Gerontol.* 2016;80:57–69.
57. Griñán-Ferré C, Puigoriol-Illamola D, Palomera-Ávalos, V. et al. Environmental enrichment modified epigenetic mechanisms in SAMP8 mouse hippocampus by reducing oxidative stress and inflammation and achieving neuroprotection. *Front. Aging Neurosci.* 2016;8:1–12.
58. Gao L, Tian S, Gao H, Xu Y. Hypoxia increases Abeta-induced tau phosphorylation by calpain and promotes behavioral consequences in AD transgenic mice. *J. Mol. Neurosci.* 2013;51:138–147.
59. Kimura T, Ishiguro K, Hisanaga S. Physiological and pathological phosphorylation of tau by Cdk5. *Front. Mol. Neurosci.* 2014;7:1–10.
60. Keller B, García-Sevilla JA. Regulation of hippocampal Fas receptor and death-inducing signaling complex after kainic acid treatment in mice. *Prog. Neuropsychopharmacol. Biol. Psychiatry.* 2015;3:63:54–62.
61. Cheng EH, Wei MD, Weiler S, Flavell RA, Mak TW, Lindster T, Korsmeyer SJ. BCL-2, BCL-X(L) sequester BH3 domain-only molecules preventing BAX- and BAK-mediated mitochondrial apoptosis. *Mol. Cell.* 2001;8:705–711.
62. Martin LJ. Mitochondrial and Cell Death Mechanisms in Neurodegenerative Diseases. *Pharmaceuticals.* 2010;3:839–915.
63. Sweatt JD. The neuronal MAP kinase cascade: a biochemical signal integration system subserving synaptic plasticity and memory. *J Neurochem.* 2001;76:1–10.
64. Hardingham GE, Bading H. Synaptic versus extrasynaptic NMDA receptor signalling: implications for neurodegenerative disorders. *Nat. Rev. Neurosci.* 2010;11:682–696.
65. Imajo M, Tsuchiya Y, Nishida E. Regulatory mechanisms and functions of MAP Kinase signalling pathways. *IUBMB Life* 2006;58: 312–317.
66. Cruz CD, Cruz F. The ERK 1 and 2 pathway in the nervous system: from basic aspects to possible clinical applications in pain and visceral dysfunction. *Curr. Neuropharmacol.* 2007;5:244–252.
67. Hyman BT, Elvhage TE, Reiter J. Extracellular signal regulated kinases. Localization of protein and mRNA in the human hippocampal formation in Alzheimer's disease. *Am. J. Pathol.* 1994;144: 565–572.

68. Russo C, Dolcini V, Salis S, Venezia V, Zambrano N, Russo, T, Schettini G. Signal transduction through tyrosine-phosphorylated C-terminal fragments of amyloid precursor protein via an enhanced interaction with Shc/Grb2 adaptor proteins in reactive astrocytes of Alzheimer's disease brain. *J. Biol. Chem.* 2002; 277: 35282-35288.
69. Kulich SM, Chu CT. Sustained extracellular signal-regulated kinase activation by 6-hydroxydopamine: implications for Parkinson's disease. *J. Neurochem.* 2001;77:1058-1066.
70. Montolio M, Gregori-Puigjané E, Pineda D, Mestres J, Navarro P. Identification of small molecule inhibitors of amyloid  $\beta$ -induced neuronal apoptosis acting through the imidazoline I(2) receptor. *J. Med. Chem.* 2012;55(22):9838-46.
71. Zhang F, Ding T, Yu L, Zhong Y, Dai H, Yan M. Dexmedetomidine protects against oxygen-glucose deprivation-induced injury through the I2 imidazoline receptor-PI3K/AKT pathway in rat C6 glioma cells. *J Pharm Pharmacol.* 2012;64(1):120-7.
72. Xuanfei L, Hao C, Zhujun Y, Yanming L, Jianping. Imidazoline I2 receptor inhibitor idazoxan regulates the progression of hepatic fibrosis via Akt-Nrf2-Smad2/3 signaling pathway. *Oncotarget.* 2017;8(13):21015-21030.
73. García-Fuster, MJ, Miralles, A, and García-Sevilla, JA. Effects of opiate drugs on Fas-Associated Protein with Death Domain (FADD) and effector caspases in the rat brain: Regulation by the ERK1/2 MAP kinase pathway. *Neuropsychopharmacology* 2007;32:399-411.
74. Ramos-Miguel A, García-Fuster MJ, Callado LF, La Harpe R, Meana JJ, García-Sevilla JA. Phosphorylation of FADD (Fas-associated death domain protein) at serine 194 is increased in the prefrontal cortex of opiate abusers: relation to mitogen activated protein kinase, phosphoprotein enriched in astrocytes of 15 kDa, and Akt signaling pathways involved in neuroplasticity. *Neuroscience* 2009;161:23-38.
75. Papaliagkas V, Anogianaki A, Anogianakis G, Ilonidis G. The proteins and the mechanisms of apoptosis: A mini-review of the fundamentals. *Hippokratia* 2007;11:108-113.
76. Ramos-Miguel A, García-Sevilla JA, Barr A. et al. Decreased cortical FADD protein is associated with clinical dementia and cognitive decline in an elderly community sample. *Mol. Neurodegener.* 2017;12:26.
77. Chinnaiyan AM, O'Rourke K, Tewari M, Dixit VM. FADD, a novel death domain-containing protein, interacts with the death domain Fas and initiates apoptosis. *Cell.* 1997;81:505-512.
78. Scott FL, Stec B, Pop C, et al. The Fas-FADD death domain complex structure unravels signalling by receptor clustering. *Nature* 2009; 457:1019-1022.
79. Alappat EC, Feig C, Boyerinas B. et al. Phosphorylation of FADD at serine 194 by CKI $\alpha$  regulates its nonapoptotic activities. *Mol. Cell.* 2005;19:321-332.
80. O'Brien RJ, Wong PC. Amyloid precursor protein processing and Alzheimer's disease. *Annu. Rev. Neurosci.* 2011;34:185-204.
81. Gralle M, Botelho MG, Wouters FS. Neuroprotective secreted amyloid precursor protein acts by disrupting amyloid precursor protein dimers. *J. Biol. Chem.* 2016; 284:15016-15025.
82. Lichtenthaler SF. Alpha-secretase cleavage of the amyloid precursor protein: proteolysis regulated by signaling pathways and protein trafficking. *Curr. Alzheimer Res.* 2012;9:165-177.
83. El-Amouri SS, Zhu H, Yu J, Marr R, Verma IM, Kindy MS. Neprilysin: An Enzyme Candidate to Slow the Progression of Alzheimer's Disease. *Am. J. Pathol.* 2008;172:1342-1354.